PI4P-signaling pathway for the synthesis of a nascent membrane structure in selective autophagy

Shun-ichi Yamashita, Masahide Oku, Yuko Wasada, Yoshitaka Ano, and Yasuyoshi Sakai

Division of Applied Life Sciences, Graduate School of Agriculture, Kyoto University, Sakyo-ku, Kyoto 606-8502, Japan

Phosphoinositides regulate a wide range of cellular activities, including membrane trafficking and biogenesis, via interaction with various effector proteins that contain phosphoinositide binding motifs. We show that in the yeast *Pichia pastoris*, phosphatidylinositol 4′-monophosphate (PI4P) initiates de novo membrane synthesis that is required for peroxisome degradation by selective autophagy and that this PI4P signaling is modulated by an ergosterol-converting PpAtg26 (autophagy-related) protein harboring a novel PI4P binding GRAM (glucosyltransferase, Rab-like GTPase activators, and myotubularins) domain. A phosphatidylinositol-4-OH kinase, PpPik1, is the primary source of PI4P. PI4P concentrated in a protein–lipid nucleation complex recruits PpAtg26 through an interaction with the GRAM domain. Sterol conversion by PpAtg26 at the nucleation complex is necessary for elongation and maturation of the membrane structure. This study reveals the role of the PI4P-signaling pathway in selective autophagy, a process comprising multistep molecular events that lead to the de novo membrane formation.

Introduction

Phosphoinositides serve as important regulators in cellular membrane dynamics and are concentrated at the specific subcellular locations. For instance, phosphatidylinositol 3′-monophosphate (PI3P), phosphatidylinositol 4′-monophosphate (PI4P), and phosphatidylinositol 4′,5′-bisphosphate are enriched in early endosomes, the Golgi apparatus, and the plasma membrane, respectively (De Matteis and Godi, 2004; Roth, 2004). These phosphoinositides contribute to membrane dynamics by recruiting specific downstream factors such as adaptor proteins, lipid transfer proteins, and components of the endosomal sorting complex required for transport (Hanada et al., 2003; Raiborg et al., 2003).

In contrast to their well-known functions in membrane dynamics of authentic organelles, only the PI3P pathway has been implicated in the phosphoinositide signaling of the autophagic processes. PI3P appears to be responsible for two distinct steps during autophagy, the de novo synthesis of the autophagosome and its fusion with vacuole/lysosome (Kihara et al., 2001; Nice et al., 2002; Wurmser and Emr, 2002; Ano et al., 2005). An autophagy-specific phosphatidylinositol-3-OH kinase (PI3K) complex, containing Atg14 in addition to Vps30 (Atg6) and Vps15, was first identified in budding yeast (Kihara et al., 2001). The potential role of other phosphoinositides in the autophagic pathway is not presently known.

We examine the selective degradation of peroxisomes through autophagy (termed pexophagy) in *Pichia pastoris*. The transient formation of a cup-shaped double-membrane structure (the micropexophagy-specific membrane apparatus [MIPA]) during micropexophagy on the cytosolic side of the peroxisome surface is crucial for the incorporation of the peroxisome into a vacuole (Mukaiyama et al., 2004; Farre and Subramani, 2004). Using fluorescence microscopy together with the MIPA marker protein PpAtg8, we examined the spatiotemporal formation of the MIPA, including its characteristic shape, size, and localization (Mukaiyama et al., 2004). As many molecular components are shared between autophagy and pexophagy, pexophagosomes and MIPAs are proposed to be synthesized de novo by a common mechanism.

In the present study, we demonstrate that PI4P (generated by PpPik1 and PpLsb6) is necessary for the formation of the membrane structure of the MIPA by revealing a novel PI4P-signaling mechanism necessary for pexophagy. To investigate how PpAtg26, a UDP-glucose:sterol glucosyltransferase having a GRAM (glucosyltransferase, Rab-like GTPase activators, and myotubularins) domain (Oku et al., 2003), contributes to pexophagy, we examined the consequences of GRAM domain–deleted

S. Yamashita and M. Oku contributed equally to this work.

Correspondence to Yasuyoshi Sakai: ysakai@kais.kyoto-u.ac.jp

M. Oku's present address is National Institute for Basic Biology, Okazaki 444-8585, Japan.

Abbreviations used in this paper: GRAM, glucosyltransferase, Rab-like GTPase activators, and myotubularins; MIPA, micropexophagy-specific membrane apparatus; PAS, preautophagosomal structure; PBD, phosphoinositide binding domain; PH, pleckstrin homology; PI3K, phosphatidylinositol-3-OH kinase; PI3P, phosphatidylinositol 3′-monophosphate; trGRAM, truncated GRAM; UBD, UDP-sugar binding domain.

The online version of this article contains supplemental material.

The Journal of Cell Biology, Vol. 173, No. 5, June 5, 2006 709–717
http://www.jcb.org/cgi/doi/10.1083/jcb.200512142

derivatives. The PpAtg26-GRAM domain binds to PI4P. We used these mutants lacking the GRAM domain to implicate this enzyme as an effector of PI4P signaling in pexophagy and to dissect the steps of its action in the membrane formation. The present results indicate that recruitment of PpAtg26 to the nucleation complex is required for the membrane elongation step but not for the nucleation of other Atg proteins. In addition, the sterol-conversion activity of PpAtg26 is essential for membrane elongation and contributes to forming the MIPA.

Results

PpAtg26 GRAM domains bind to PI4P

The pathological and clinical importance of GRAM domains is supported by a report documenting that some myopathy patients have mutations within the GRAM domains of myotubularins (Fig. 1 A; Doerks et al., 2000). GRAM domains from the myotubularins bind to phosphoinositides (Berger et al., 2003; Tsujita et al., 2004), but these display low homology to the GRAM domain of Atg26 (Fig. 1 A; Doerks et al., 2000).

First, to explore which phospholipids might bind to the GRAM domain of PpAtg26, we compared the binding properties of the GRAM domains from yeast PpAtg26 ($GRAM_{Atg26}$ and truncated GRAM [trGRAM]–PH) with that from human myotubularin ($GRAM_{Mtm1}$; Fig. 1 B). In a protein lipid overlay assay, both PpAtg26 domains bound to PI4P with the highest affinity (Fig. 1 C). The binding of $GRAM_{Atg26}$ to PI4P was also confirmed by surface plasmon resonance analysis (Fig. 1 D; K_d = 6.9 nM). The $GRAM_{Atg26}$ domain was found to have less but substantial binding activity to phosphatidylinositol

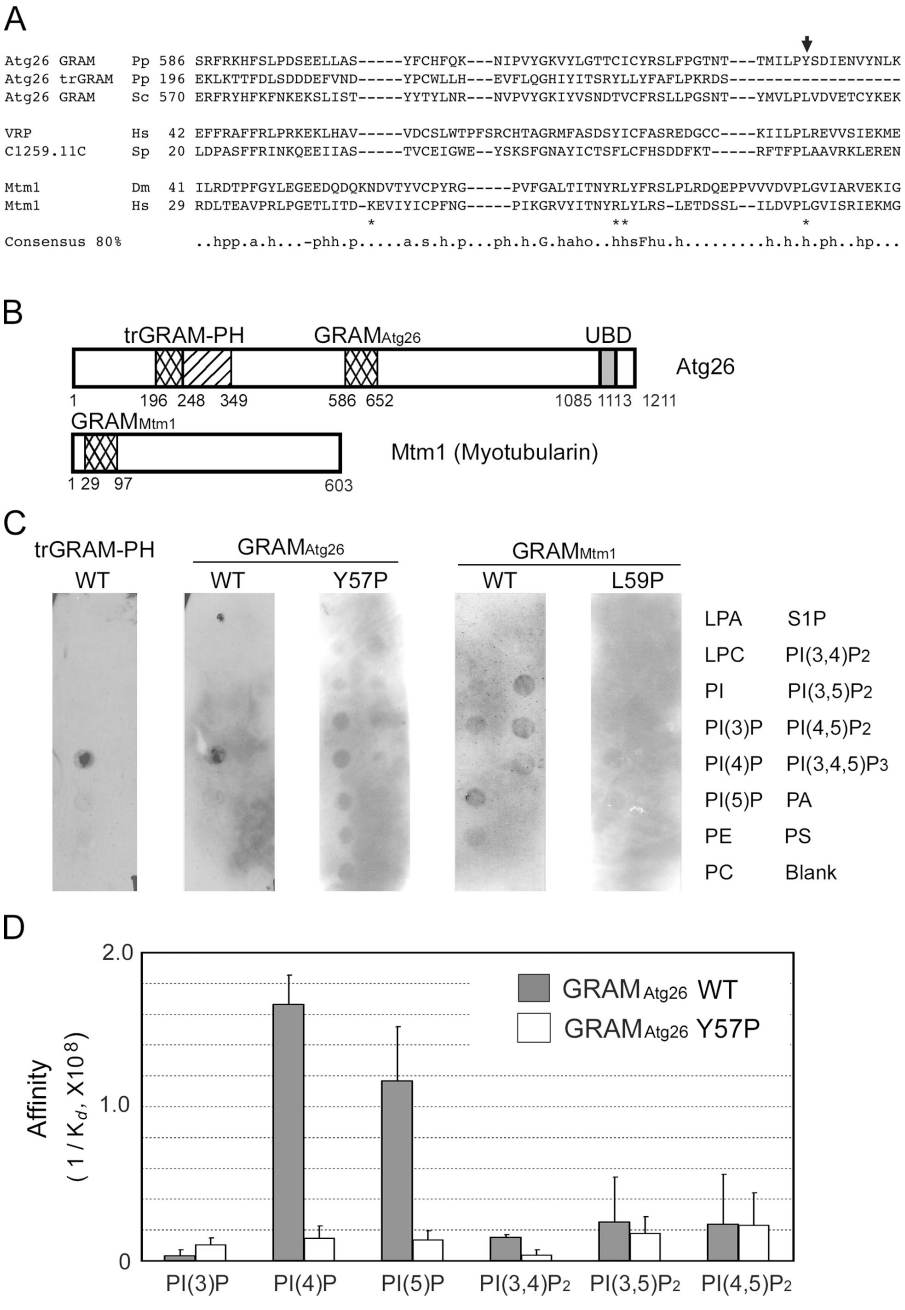

Figure 1. **The $GRAM_{Atg26}$ domain is sufficient for specific binding to PI4P.** (A) Sequence alignment of GRAM domains from various organisms: Pp, *P. pastoris*; Sc, *S. cerevisiae*; Hs, *Homo sapiens*; Sp, *Schizosaccharomyces pombe*; Dm, *Dictyostelium discoideum* (Doerks et al., 2000). The sequences are from Atg26 UDP-glucose:sterol glucosyltransferases (top), Rab-like GTPase activators (middle), and myotubularins (bottom), respectively. An arrow indicates the amino acid residues mutated in this study that correspond to $GRAM_{Atg26}$ Y57 and $GRAM_{Mtm1}$ L59. The mutations in the GRAM domain of human Mtm1 are labeled with asterisks below the sequence (Doerks et al., 2000). The highly conserved consensus sequence is shown below: h, hydrophobic; p, polar; a, aromatic; u, tiny; s, small; o, alcoholic; −, negatively charged residues. (B) Schematic representations of PpAtg26 and human Mtm1. The numbers indicate amino-acid residues. (C) Protein lipid overlay assays for detecting the binding of the indicated lipids to the trGRAM-PH, $GRAM_{Atg26}$, and $GRAM_{Mtm1}$ domains. Fusion proteins containing the designated domains with normal (WT) or point-mutated (Y57P or L59P) amino-acid sequences were purified and assayed with PIP Strips. LPA, lysophosphatidic acid; S1P, sphingosine-1-phosphate; LPC, lysophosphatidylcholine; PI, phosphatidylinositol; PA, phosphatidic acid; PE, phosphatidylethanolamine; PS, phosphatidylserine; PC, phosphatidylcholine. (D) The purified $GRAM_{PpAtg26}$ fusion proteins used in C were subjected to surface plasmon resonance analysis using a BIACORE 2000 system. The reciprocal values of the dissociation constants (K_d) for the interaction of fusion proteins and the phosphoinositides are presented. The error bars indicate standard deviations.

5′-monophosphate (PI5P). However, the yeast cells do not contain PI5P. Neither $GRAM_{Atg26}$ nor trGRAM-PH bound to ergosterol or ergosterol glucoside, the substrate and the product of reaction catalyzed by PpAtg26. $GRAM_{Mtm1}$ exhibited broader binding specificities than $GRAM_{Atg26}$ as reported previously (Berger et al., 2003; Tsujita et al., 2004; Fig. 1 C). The binding specificity of $GRAM_{Atg26}$ was confirmed with a protein-liposome sedimentation assay (unpublished data). These data demonstrate that $GRAM_{Atg26}$ binds to PI4P but not to other phosphoinositides present in yeast cells, such as PI3P, phosphatidylinositol 3′,5′-bisphosphate, or phosphatidylinositol 4′,5′-bisphosphate.

Next, we generated a mutant version of $GRAM_{Atg26}$ that carried a Y57P amino acid substitution. This mutation corresponds to one of the substitutions found in myopathy patients (Mtm1 L59P; Fig. 1 A). The $GRAM_{Atg26}$ Y57P mutation caused a pexophagic defect (Oku et al., 2003). Both the $GRAM_{Atg26}$ Y57P and $GRAM_{Mtm1}$ L59P substitutions eliminated the high-affinity binding and specificity of the GRAM domains (Fig. 1, C and D), thereby linking the biochemical properties of these GRAM domains to the mutant phenotypes.

Phosphatidylinositol 4-kinases are required for pexophagy

To determine the role of PI4Ks in MIPA formation and pexophagy, we generated three *P. pastoris* strains, one mutant for each one of the PI4Ks—PpPik1, PpStt4, and PpLsb6. To construct *Pppik1* and *Ppstt4* mutants, serine residues conserved in the putative catalytic site of PI4Ks (S994 for PpPik1 and S1816 for PpStt4) were substituted with phenylalanine (Walch-Solimena and Novick, 1999).

The *Pppik1* and *Ppstt4* strains exhibited growth defects, whereas *Pplsb6* cells displayed a normal growth rate. These phenotypes are similar to those reported for the *Saccharomyces cerevisiae* PI4K mutants (Audhya et al., 2000; Han et al., 2002). Inositol labeling experiments indicated that in comparison to wild-type cells the size of the intracellular PI4P pool was reduced by ∼11, 30, and 45% in *Pplsb6*, *Pppik1*, and *Ppstt4* mutants, respectively (Fig. 2 A).

We assessed pexophagy in these PI4K mutants by examining peroxisomal alcohol oxidase activity (Fig. 2 B). This enzyme is degraded through pexophagy along with other components of the peroxisome (Tuttle and Dunn, 1995). In this assay, persistent alcohol oxidase activity resulting from impaired pexophagy produces a colored colony (Sakai et al., 1998). In *Ppstt4* cells, pexophagy occurred as rapidly as in wild-type cells, whereas the pexophagic activity was abrogated in *Pppik1* cells and attenuated in *Pplsb6* cells (Fig. 2 B).

Next, we followed the formation of the membrane structure of the MIPA in these pexophagy-defected PI4K mutants to explore whether PI4P signaling is essential for the formation of the membrane structure. As PpAtg8 is targeted specifically to the MIPA through a ubiquitin-like conjugation, a YFP-labeled PpAtg8 was used as a marker for the MIPA. 1 h after inducing pexophagy, ∼7% of the wild-type cells exhibited a cup-shaped fluorescent signal characteristic of the MIPA (Fig. 2, C and D). The low frequency of observable MIPA is due in part to its transient nature; this membrane structure is formed only just before the incorporation of the peroxisome into the vacuole, after which it is destroyed (Mukaiyama et al., 2004). Under these conditions, *Pppik1* cells did not exhibit any cup-shaped YFP-PpAtg8 fluorescence; instead, small fluorescent puncta were proximal to the peroxisomes (Fig. 2 C). *Pplsb6* mutant cells showed cup-shaped MIPA fluorescent signals, but the percentage of cells containing these structures was lower than that seen in the wild-type cells (Fig. 2, C and D). These results correlate well with the data obtained from the alcohol oxidase assay (Fig. 2 B), demonstrating a novel and critical role for PI4Ks in the formation of the membrane structure during pexophagy.

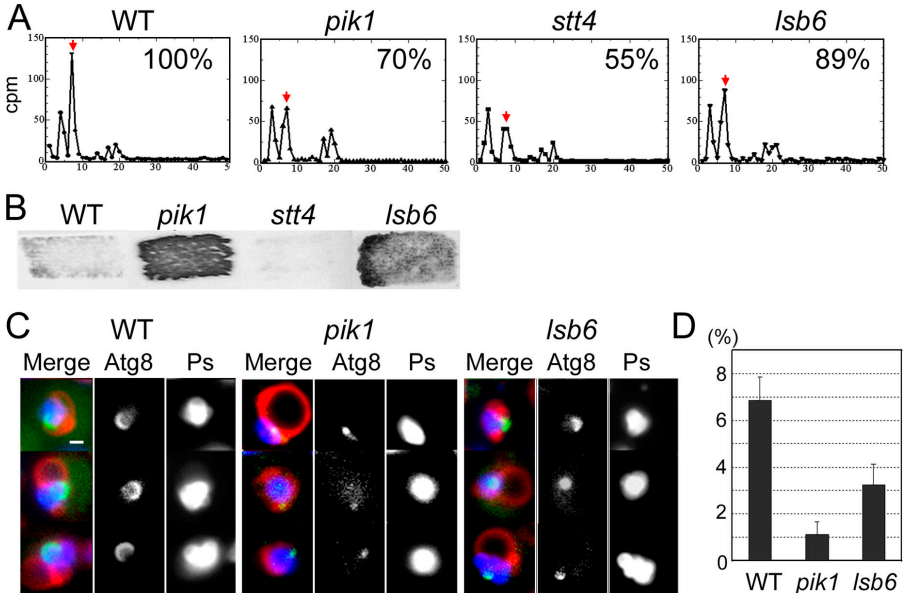

Figure 2. **PI4K is necessary for assembly of the MIPA.** (A) Intracellular phosphoinositide quantification. Lipids from the designated strains were assayed by HPLC (see Materials and methods). Data were normalized to PI3P levels (cpm value of the first peak). The arrows mark the peaks representing PI4P. The inset percentage values are the ratios calculated for the PI4P content to the PI4P level detected in the wild-type (WT) strain. (B) Peroxisomal alcohol oxidase activity. The strains used in A were subjected to pexophagic conditions; alcohol oxidase activities were stained in situ. (C) Fluorescence microscopy of the PI4K mutants. Strains carrying YFP-PpAtg8 and CFP-labeled peroxisomes were analyzed after shifting to pexophagic conditions. The merged images comprise the green PpAtg8 signals (shown independently in the middle rows), the blue peroxisome (Ps) signals (right rows), and the red vacuolar membrane stained with FM4-64. Bar, 1 μm. (D) MIPA formation after pexophagy induction was assessed by determining the ratio of the number of cup-shaped structures to the number of peroxisomal clusters. The error bars show standard deviations.

PI4P is concentrated in the MIPA

YFP-GRAM$_{Atg26}$ was used as a probe to visualize the intracellular distribution of PI4P. In a CHO cell line, YFP-GRAM$_{Atg26}$ produced a typical Golgi-like fluorescence that overlapped with the fluorescence pattern of the Golgi marker, BODYPY TR C5-ceramide (Fig. S1, available at http://www.jcb.org/cgi/content/full/jcb.200512142/DC1). As GRAM$_{Atg26}$ specifically binds to PI4P and the Golgi is a PI4P-containing organelle (Roth, 2004), our observation verified that the expressed GRAM probe recognizes the intracellular PI4P in a heterologous host.

In *P. pastoris*, YFP-GRAM$_{Atg26}$ generated peculiar ring-shaped fluorescence under pexophagic conditions and interfered with the localization of CFP-PpAtg8 to the MIPA (Fig. 3 A). The shape and localization of the YFP-GRAM$_{Atg26}$ fluorescent signal, together with subcellular fractionation experiments (Fig. 3 B), support the conclusion that YFP-GRAM$_{Atg26}$ localizes to the Golgi apparatus or Berkeley body. Mislocalization of CFP-PpAtg8 to MIPA may be due to the secondary effect of disordered function of the Golgi apparatus.

We speculated that the inhibition of MIPA formation resulted from the masking of functional PI4P by the overexpressed GRAM$_{Atg26}$. To eliminate this inhibition, we performed subcellular fractionation experiments of the MIPA-formed cells and probed the PI4P pool with a GRAM domain fusion protein (Fig. 3 B). Purified GST-GRAM$_{Atg26}$-CFP proteins (Fig. 1, WT or Y57P) were incubated with membrane fractions isolated from pexophagy-induced cells expressing HA-tagged PpAtg8. Sucrose density gradient ultracentrifugation in combination with immunoblot analyses was performed on the subsequent fractions.

The bulk of GRAM$_{Atg26}$ protein (Fig. 3 B, closed rectangles) was present in two peaks within the range of the high-density fractions (fractions 1–4) and the low-density fractions (fractions 10–12; Fig. 3 B). HA-PpAtg8 (a MIPA marker; Fig. 3 B, open circles) signal exclusively distributed to the high-density fractions (fractions 1–4) and colocalized with one of the GRAM$_{Atg26}$ peaks. The peaks in the low-density fractions overlapped with the Kex2-positive fractions (Fig. 3 B, asterisks), consistent with PI4P in the Golgi apparatus (Levine and Munro, 2002). We conclude that GRAM$_{Atg26}$ targeting to the membrane fraction was PI4P specific and that the high-density PpAtg8-positive fractions also contained PI4P.

The GRAM$_{Atg26}$Y57P mutant protein (Fig. 3 B, open rectangles) was not enriched in the high-density fractions, consistent with the notion that the GRAM$_{Atg26}$ targets to the high-density fractions through binding PI4P. The GRAM$_{Atg26}$Y57P mutant protein was present in the low-density fractions, but its distribution was broader than that of the GRAM$_{Atg26}$ and included higher density fractions. As the GRAM$_{Atg26}$Y57P mutant protein does not bind PI4P specifically but retains weak and nonspecific PI binding activities (Fig. 1, C and D), the distribution of the GRAM$_{Atg26}$Y57P mutant protein may result from less specific binding to various PI pools in the cellular membranes. The enrichment of PI4P in PpAtg8-positive structures also was confirmed by in situ application of CFP-GRAM$_{Atg26}$ to permeabilized cells expressing YFP-PpAtg8 (unpublished data). Thus, the formed PpAtg8-positive structures, i.e., MIPAs, are rich in PI4P.

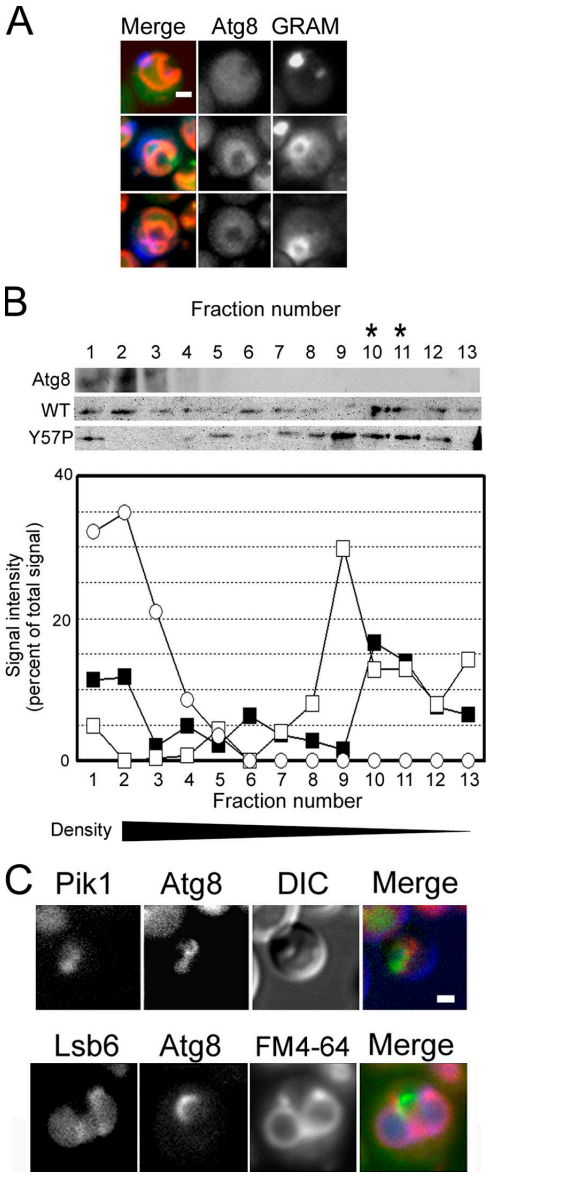

Figure 3. **The MIPA is a PI4P-enriched compartment.** (A) In vivo GRAM$_{Atg26}$ expression perturbs intact MIPA formation. The YFP-GRAM$_{Atg26}$ fusion protein was expressed in cells expressing CFP-PpAtg8. The cells were shifted to pexophagic conditions and examined by fluorescence microscopy. The merged image comprises the vacuolar membrane stained with FM4-64 (red), CFP-PpAtg8 fluorescence (green), and YFP-GRAM fluorescence (blue). The CFP-PpAtg8 and YFP-GRAM fluorescence patterns are also shown individually (middle and right, respectively). Note that the CFP-PpAtg8 failed to produce a cup-shaped fluorescent signal, and YFP-GRAM formed puncta or ring-shaped structures. (B) Sucrose density gradient fractionation from cell-free extracts after incubation with either wild-type (WT) or mutant (Y57P) purified GRAM$_{Atg26}$ protein. Each fraction was subjected to immunoblot analysis detecting PpAtg8 (open circle) and GRAM proteins (wild-type GRAM, filled rectangle; mutated GRAM, open rectangle). The signal intensity for each band was determined and plotted. The membrane was reused for detecting Kex2, and the range of fractions with detectable signal is indicated with asterisks. (C) Fluorescent microscopy of the PI4Ks involved in pexophagy. PpPik1 (Pik1) and PpLsb6 (Lsb6) were expressed as fusions to CFP. Localizations were compared with YFP-PpAtg8 (Atg8), and the image of differential interference contrast (DIC) microscopy or a vacuolar membrane marker (FM4-64) under micropexophagic conditions. The superimposed images are also shown. Bars, 1 μm.

Both PI4Ks (PpPik1 and PpLsb6) involved in the membrane formation did not colocalize with YFP-PpAtg8, the MIPA marker (Fig. 3 C). CFP-PpPik1 exhibited a punctate distribution that did not overlap with the cup-shaped YFP-PpAtg8 fluorescence of the MIPA. CFP-PpLsb6 resided on the vacuolar membrane (and lumen), as reported for ScLsb6 (Fig. 3 C; Han et al., 2002). These observations are consistent with PI4P migrating from the sites of their production to the nascent MIPA.

PI4P is dispensable for the localization of other Atg proteins

Studies of the localization of Atg proteins in *S. cerevisiae* reveal that multiple Atg proteins localize to a single puncta in the vicinity of the vacuole before autophagosome formation that is referred to as the preautophagosomal structure (PAS; Suzuki et al., 2001; Noda et al., 2002). The formation of PAS appears to be a prerequisite for autophagic membrane formation. Our *P. pastoris* studies have also identified a punctate structure containing several Atg proteins (PpAtg8, PpAtg5, PpAtg16, and PpAtg26) before the MIPA formation (unpublished data). Lipidation of PpAtg8 through a ubiquitin-like conjugation system (PpAtg4, PpAtg7, and PpAtg3) is necessary for PpAtg8 to localize to punctuate structures (Mukaiyama et al., 2004), consistent with these PpAtg8 puncta–containing protein–lipid complexes.

In the *Pppik1* cells, the YFP-PpAtg8 puncta colocalized with PpAtg16- and PpAtg5-CFP (Fig. 4 B), two Atg proteins concentrated in PAS in *S. cerevisiae* (Noda et al., 2002). In contrast, the YFP-PpAtg8 puncta in the *Pppik1* cells did not overlap with CFP-PpAtg26 (Fig. 4 B). Thus, PI4P recruits PpAtg26 but is dispensable for the localization of at least three Atg proteins (PpAtg8, PpAtg5, and PpAtg16) to these punctate structures.

Disruption of another responsible PI4K, PpLsb6, caused a less prominent phenotype (Fig. 4 B). The percentage of the *Pplsb6* cells possessing MIPAs was reduced in comparison to

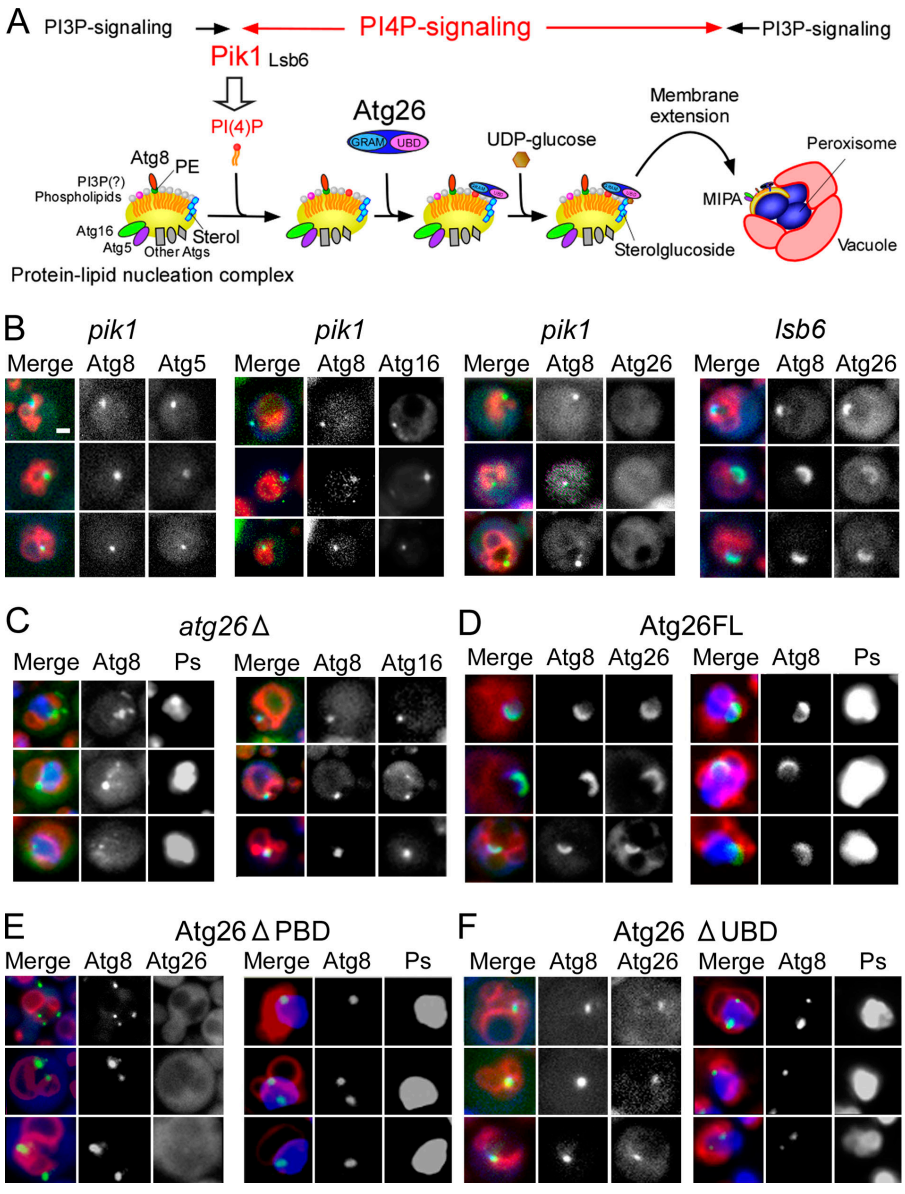

Figure 4. **PpAtg26 mediates PI4P signaling required for the de novo formation of the membrane structure.** (A) A model of PI4P signaling in membrane structure formation during pexophagy. In the nucleation step, a precursor protein–lipid complex is assembled from multiple Atg proteins (containing at least lipidated Atg8, Atg5, and Atg16, and possibly PI3P). PpPik1 and PpLsb6 supply PI4P, which elevates the concentration of PI4P at the nucleation complex. Subsequently, PpAtg26 is recruited to the nucleation complex through binding of its GRAM domains to PI4P. Ergosterol conversion by the recruited PpAtg26 promotes elongation of the membrane structure, leading to the formation of a MIPA. PI3P signaling regulates autophagic processes, including nucleation and fusion of the membrane structure with the vacuole, e.g., PpAtg24 as an effector (Ano et al., 2005). (B) Fluorescence microscopy of the PI4K mutant strains. *Pppik1* or *Pplsb6*Δ cells expressing the indicated fluorescent fusion proteins were examined under the pexophagic conditions. (C) Fluorescence imaging of the *Ppatg26*Δ strain. The *Ppatg26*Δ cells possessing YFP-PpAtg8 and either CFP-PpAtg16 (Atg16) or CFP-labeled peroxisomes (Ps) were observed under micropexophagic conditions. (D–F) Fluorescence microscopy of the cells with PpAtg26 variants. The *Ppatg26*Δ cells were rescued with full-length PpAtg26 (Atg26FL; D), PBD-deleted PpAtg26 (Atg26ΔPBD; E), or UBD-deleted PpAtg26 (Atg26ΔUBD; F). Either PpAtg26 (left) or peroxisomes (Ps) were fluorescently labeled for microscopy to examine cells under pexophagic conditions.

the wild-type strain (Fig. 2 D), but the observed MIPAs contained CFP-PpAtg26, unlike *Pppik1* cells. These results are consistent with our findings in the pexophagy and MIPA formation assay (Fig. 2), where PpPik1 was a major contributor to pexophagy but PpLsb6 was not.

PpAtg26 acts downstream of PI4K at the membrane elongation step

In *ATG26* mutant cells (*Ppatg26*Δ), YFP-PpAtg8 fluorescence did not develop into a cup-shaped MIPA structure but rather colocalized in puncta with PpAtg16-CFP (Fig. 4 C). Thus, PpAtg26 is required for MIPA formation. In addition to a phosphoinositide binding domain (PBD) comprising GRAM, trGRAM, and a pleckstrin homology (PH) domain, PpAtg26 contains a catalytic region including a UDP-sugar binding domain (UBD) that is necessary for the catalysis of ergosterol and UDP-glucose to ergosterol glucoside (Warnecke et al., 1999). To analyze further the role of PpAtg26 in MIPA formation, we introduced constructs into *Ppatg26*Δ cells that encode one of several CFP-PpAtg26 variants, including a full-length PpAtg26 (CFP-PpAtg26FL; Fig. 4 D), a PpAtg26 mutant protein lacking the PBD (aa 198–652; CFP-PpAtg26ΔPBD; Fig. 4 E), and a PpAtg26 variant missing the UBD (aa 1085–1113; CFP-PpAtg26ΔUBD; Fig. 4 F).

CFP-PpAtg26FL rescued the pexophagic defect of the *Ppatg26*Δ mutant cells; it colocalized with cup-shaped YFP-PpAtg8 fluorescence of MIPAs (Fig. 4 D). In contrast, expression of CFP-PpAtg26ΔPBD did not yield the cup-shaped YFP-PpAtg8 fluorescence. CFP-PpAtg26ΔPBD was dispersed throughout the cytosol (Fig. 4 E). We conclude that PI4P binding by the PBD is essential for the PpAtg26 localization to the Atg8-positive puncta proximal to peroxisomes, a prerequisite for the membrane elongation necessary to form the MIPA.

Deletion of each domain within the PBD (trGRAM, PH, or GRAM) produced a similar pattern of PpAtg8 fluorescence to the overall PBD deletion; i.e., only fluorescent puncta were observed (Fig. S2, available at http://www.jcb.org/cgi/content/full/jcb.200512142/DC1). The PH domain–deleted mutant had the most severe phenotype, as we did not observe any colocalization with YFP-PpAtg8 (Fig. S2). The CFP-PpAtg26 variants lacking either the GRAM domain or trGRAM colocalized with PpAtg8 puncta less frequently than CFP-PpAtg26FL (Fig. 4 D and Fig. S2). These deletion constructs confirm the important role for each domain in MIPA formation, consistent with previous experiments (Oku et al., 2003). In addition, we conclude that these PI4P binding regions function cooperatively to recruit PpAtg26 to punctual structures.

Overexpression of CFP-PpAtg26ΔUBD did not restore the sterol-converting activity to the *Ppatg26*Δ mutant cells as determined by thin-layer chromatography (Fig. S3, available at http://www.jcb.org/cgi/content/full/jcb.200512142/DC1). This strain did not exhibit the cup-shaped YFP-PpAtg8 fluorescence but did have YFP-PpAtg8 puncta (Fig. 4 F). In contrast to CFP-PpAtg26ΔPBD expression (Fig. 4 E), these puncta colocalized with CFP-PpAtg26ΔUBD fluorescence (Fig. 4 F). We conclude that PpAtg26-dependent ergosterol conversion at the assembly site of multiple Atg proteins is necessary for maturation and elongation of the membrane structure to form the MIPA.

Discussion

The present study examines a novel PI4P-signaling pathway for the formation of the membrane structures required for pexophagy. Although our previous study identified PpAtg26 as a factor necessary for pexophagy and demonstrated the functional importance of its GRAM domain in pexophagy (Oku et al., 2003), neither the role of Atg26 in the formation of the membrane structure nor the biochemical function of the GRAM domain was made clear. Here, we demonstrate that the GRAM domains of PpAtg26 bind specifically to PI4P. We propose that the GRAM domain is indeed a phosphoinositide binding motif that is conserved from yeast to higher eukaryotes. This finding prompted us to study PI4P signaling during pexophagy. Indeed, among three PI4Ks (PpPik1, PpStt4, and PpLsb6) present in yeast cells, mutations in PpPIK1 and PpLSB6 impair pexophagy. We consider this direct evidence that PI4P signaling is involved in pexophagy, especially in the formation of the membrane structure.

The formation of the membrane structure during pexophagy involves three distinct steps (Fig. 4 A): (1) PI4P (predominantly synthesized by PpPik1) concentrates in the nucleation complex, where multiple Atg proteins (including lipidated PpAtg8) assemble; (2) PpAtg26 is recruited to the nucleation complex through an interaction between PI4P and the GRAM domain; and (3) sterol conversion at the nucleation site triggers elongation and maturation of the membrane structure. Although the maturation and elongation of the membrane structure are defective in the PI4K or PpAtg26 mutant strains, many Atg proteins, except PpAtg26, assembled at the peroxisomal surface normally. In contrast, in *S. cerevisiae* strains deficient in the PI3 kinase (Vps34) complex (Suzuki et al., 2001), the nucleation step of autophagosome formation is impaired, and there is a marked deficiency in the localization of multiple Atg proteins at the PAS (Noda et al., 2002; Farre and Subramani, 2004). For example, we observed multiple YFP-PpAtg8 puncta dispersed in the cytosol of the *Ppvps15* mutant (unpublished data) in contrast to a single punctum in the *Pppik1* mutant, suggesting that proper formation of the MIPA precursor at the peroxisomal surface requires PI3P signaling. These findings support a nucleation and elongation/maturation model of autophagosome assembly (Noda et al., 2002; Farre and Subramani, 2004). We propose that each step of the de novo membrane formation during pexophagy is regulated by two distinct phosphoinositides—PI3P and PI4P.

To date, most of the molecular events exerted by PI4P signaling in yeast cells are related to the Golgi apparatus (Walch-Solimena and Novick, 1999; Sciorra et al., 2005). The absolute requirement of PpPik1 for MIPA formation implicates lipid/membrane flow from Golgi-related compartments during the de novo membrane structure synthesis. Previous studies on other autophagic pathways demonstrate the contribution of the early secretory pathway (involving ER and Golgi) in autophagosome formation (Hamasaki et al., 2003; Reggiori et al., 2004). In addition, Tlg2, a syntaxin homologue Tlg2 that shuttles between the late Golgi and the endosomal membrane, is involved in a specific autophagic cytosol to the vacuole targeting

pathway for aminopeptidase I biogenesis (Abeliovich et al., 1999). Our results also support the possibility that PI4P (possibly together with other lipids) flows from the early secretory pathway to the nucleation site to form membrane structure.

In contrast to the evidence implicating PpPik1 in pexophagy, the role of PpLsb6 is not established. The *Pplsb6* mutant has no abnormalities in the growth rate or endocytosis (deduced by FM4-64 uptake). How and where PI4P synthesis by PpLsb6 contributes to pexophagy is not clear. However, considering that the formation frequency of MIPA was reduced in the *Pplsb6* mutant (Fig. 2 D), we propose that PI4P produced by PpLsb6 is transported to the nucleation complex and that this PI4P helps to recruit PpAtg26 alongside PI4P produced by PpPik1.

Although the expressed $GRAM_{Atg26}$ domain localizes to the Golgi apparatus as well as to the MIPA (Fig. 3, A and B), CFP-PpAtg26FL exclusively localized to the MIPA (Fig. 4 B). We assume that this difference results from the other PpAtg26 regions contributing to the localization of this protein, especially the PH domain. Our previous study demonstrated that PpAtg26 resides in a membrane fraction that is resistant to extraction by Triton X-100, and this property of detergent insolubility is partially dependent on the PH domain (Oku et al., 2003). Thus, the PH domain may recognize "lipid" rafts within the target membrane. The concerted actions of both the GRAM and PH domains may mediate the specific recruitment of PpAtg26 to the MIPA.

PI4P signaling recruits PpAtg26 to the nucleation complex and culminates with ergosterol conversion at a specific site. The exact functions of ergosterol conversion in the phenomenon of membrane elongation are not yet understood. However, our finding reveals a novel physiological role of sterol as a reaction substrate required for the formation of a membrane structure. Also, it is worthwhile to point out the sterol-free characteristics of autophagosome-like membranes in mammalian cells. Unlike endosomal membranes, mammalian Atg8 (LC3)-positive isolation membranes, which engulf bacteria, are resistant to the cholesterol binding toxin streptolysin O (Nakagawa et al., 2004). Although mammalian Atg26 homologues have not been identified as yet, *Dictyostelium discoideum* has an Atg26 orthologue that contains a phosphoinositide binding FYVE domain (Doerks et al., 2000). These observations may reflect a conserved mechanism of de novo membrane formation during the selective autophagy that is dependent on phosphoinositide signaling and site-specific sterol conversion.

Materials and methods

Protein–lipid binding experiments

PpAtg26 regions corresponding to aa 196–248 (trGRAM-PH), aa 586–642 ($GRAM_{Atg26}$), and the HsMtm1 region (aa 29–97; $GRAM_{Mtm1}$) were generated by PCR amplification. The amplified fragments were cloned into the pGEX6P-1 vector (GE Healthcare) to produce fusion proteins with GST and YFP. Point mutations of the tyrosine residue at position 57 of $GRAM_{Atg26}$ with a proline residue (Y57P) and the leucine residue at position 59 of $GRAM_{Mtm1}$ with a proline residue (L59P) were made with the QuikChange PCR kit (Stratagene). Protein expression in *Escherichia coli* Rosetta DE3 cells (Novagen) was induced with 0.5 mM IPTG at 20°C for 6 h. Expressed proteins were purified using glutathione Sepharose 4B (GE Healthcare) according to the manufacturer's instructions, except that DTT and Triton X-100 were omitted from the procedures. The glutathione-eluted samples were dialyzed against HBS buffer (10 mM Hepes and 150 mM NaCl, pH adjusted to 7.4) and used as a purified fusion protein in the subsequent assays. The protein lipid overlay assays were done with PIP Strips (Echelon Biosciences) using 1 μg/ml of the purified proteins in accordance with the manufacturer's instructions. Surface plasmon resonance analysis was done using a BIACORE 2000 system and Sensor chip L1 (Biacore). Liposome samples (1 mg/ml total lipid concentration) containing 60% (wt/wt) phosphatidylcholine, 19% (wt/wt) phosphatidylserine, 19% (wt/wt) cholesterol, and 2% (wt/wt) phosphoinositide were prepared by sonication (the lipids were purchased from Sigma-Aldrich). The sensor chip was coated with 3,000 RU of liposome and then coated with another 3,000 RU of liposome that lacked phosphoinositides. Samples containing 10–40 ML/ml of the purified $GRAM_{Atg26}$ fusion protein were applied to the chip, and the results were analyzed with BIAevaluation 3.0 (Biacore). The dissociation constants (K_d values) were determined from three independent experiments.

Generation of the PI4K mutants and determination of intracellular PI4P content

To generate the *Pppik1* and *Ppstt4* mutant strains, 1-kb fragments within both *P. pastoris* kinase genes (available from GenBank/EMBL/DDBJ under accession nos. AB220683 and AB221015) encoding their COOH-terminal regions were cloned into pPICZ-A (Invitrogen). Point mutations were then introduced using the QuikChange PCR kit. The plasmids were linearized and introduced into wild-type YAP0004 genome (Ano et al., 2005), resulting in the genomic replacement of PpPIK1and PpSTT4 by the mutated ORFs, the COOH-terminal region of PpPik1S994F and PpStt4S1816F, respectively. To generate the *Pplsb6* strain, the PstI–BglII fragment of the PpLSB6 ORF (available from GenBank/EMBL/DDBJ under accession no. AB220684) was cloned into pPICZ-A (Invitrogen). The resultant plasmid was digested with SnaBI and introduced into the YAP0004 strain genome to produce cells carrying two truncated forms of PpLSB6. To induce pexophagy, all of the prepared mutant strains were cultured for 15 h in synthetic methanol medium (0.75% methanol, 0.75% yeast nitrogen base without amino acids [Difco], and 100 mg/l auxotrophic amino acids) containing 0.37 MBq/ml ^{3}H-labeled *myo*-inositol (GE Healthcare) and shifted to glucose medium (2% D-glucose, 0.75% yeast nitrogen base without amino acids, and 100 mg/l auxotrophic amino acids) for 1 h. After the cells were harvested, total lipid was extracted, deacylated with methylamine, and analyzed by HPLC according to the procedure described in a previous study (Stolz et al., 1998).

Subcellular fractionation assay

3 μg of each of the purified $GRAM_{Atg26}$ fusion proteins used in the protein–lipid binding experiments was incubated at 4°C for 14 h with a 100,000 *g* pellet fraction (equivalent to 0.4 mg protein) of the PPM5011 strain (Mukaiyama et al., 2002) cell homogenate expressing HA-tagged PpAtg8. Subsequent ultracentrifugation was done essentially as described previously (Noda et al., 2000), except that 40 mM NaF was added to the lysis buffer. Each fraction was subjected to immunoblot analysis. The primary antibodies used for immunoblotting were as follows: the GRAM domains were detected with an anti-GFP rabbit polyclonal antibody (1:3,000; Invitrogen), the PpAtg8 with an anti-HA mouse monoclonal antibody (1:1,000; Boehringer), and Kex2 with an anti-Kex2 goat polyclonal antibody (1:1,000; Santa Cruz Biotechnology, Inc.). The ECL system was used for secondary detection (GE Healthcare), and bands were analyzed with MetaMorph imaging software (Universal Imaging Corp.).

Alcohol oxidase assay

The alcohol oxidase assay and fluorescence microscopy were done as described previously (Mukaiyama et al., 2004).

Fluorescence microscopy and image acquisition

Fluorescently labeled yeast cells were examined immediately after sampling under a fluorescence-inverted microscope (IX70; Olympus) equipped with a Uplan Apo 100×/1.35 oil iris objective lens using mirror/filter units U-MWIG (Olympus) for FM 4-64, U-MF2 (Olympus) filter set (XF114-2; Omega Optical, Inc.) for CFP, and U-MF2 filter set (XF104-2; Omega Optical, Inc.) for YFP. Image data were captured with a charged-coupled device camera (SenSys; PhotoMetrics) using MetaMorph. 4.6 and were saved as Photoshop files (Adobe) on a computer (Endeavor MT-4500 [Epson] with Windows [Microsoft]). The TIFF image files were transferred to another computer (G5; Macintosh), and the images were optimized for their contrast on Photoshop CS2 and compiled on Illustrator CS2 (Adobe).

In order to observe the localization of $GRAM_{Atg26}$ in mammalian CHO-K1 cells, a plasmid derived from pTRE2hyg vector (CLONTECH Laboratories, Inc.) harboring a DNA fragment encoding YFP-$GRAM_{Atg26}$ was

introduced into CHO-K1 Tet-On Cell Line (CLONTECH Laboratories, Inc.). After successive selection with hygromycin for transfected cells, doxycycline (CLONTECH Laboratories, Inc.) was applied at 1 μg/ml and incubated for 48 h to induce the expression of the fusion protein. The cells were subsequently incubated for 1 h with BODYPY TR C5-ceramide complexed to BSA (Invitrogen) in the presence of 5 μM ceramide. A confocal microscope (LSM510 META; Carl Zeiss MicroImaging, Inc.) equipped with a multiline (458, 477, 488, and 514 nm) argon ion visible lasers along with a 63× Plan-Apochromat NA 1.4 oil immersion (Carl Zeiss MicroImaging, Inc.) was used for observation of CHO cells.

The frequency of MIPA formation was determined by counting the number of cup-shaped images after YFP-PpAtg8 labeling. These values were normalized to the number of peroxisome grains labeled with CFP in the same observation area. The presented values are the mean from three separate experiments (where each count included >100 cells). CFP and NH_2-terminal 1-kb PpPik1 fragments were cloned into the pIB2 expression vector that carried a $(Ala)_7$-Gly-Ser linker sequence between the two ORFs to express the CFP-PpPik1 under glyceraldehyde-3-phosphate dehydrogenase (GAP) promoter. The resultant plasmid was excised with EcoRV and then introduced into the *P. pastoris* SA1017 strain (containing YFP-PpAtg8) to replace the NH_2-terminal region of the genomic PpPIK1. The full-length PpLSB6 ORF fused to CFP in the pIB2 expression vector was also introduced into the *P. pastoris* SA1017 strain to visualize PpLSB6. PpAtg5-CFP was expressed under the control of its own promoter cloned into pHM100 (Mukaiyama et al., 2004), and PpAtg16-CFP was expressed under the control of the GAP promoter. The plasmids encoding CFP-fused PpAtg26 and its domain-deleted derivatives were constructed in the CFP-cloned pIB4 expression vector (with alcohol oxidase promoter) as follows: PpAtg26FL, full-length ORF; PpAtg26ΔPBD, ORF lacking the region corresponding to aa 196–652; PpAtg26ΔUBD, ORF lacking the region for aa 1085–1113 (all the domain deletions were generated with the QuikChange PCR kit). Each deletion construct was expressed in a YFP-PpAtg8–harboring strain whose endogenous *PpATG26* had been disrupted by the method described previously (Oku et al., 2003).

Detection of sterol glucoside

The lipid extraction from 100 OD unit cells of each strain was done by the Bligh-Dyer method, and the thin-layer chromatography was performed as described previously (Warnecke et al., 1999). Sterol glucoside was detected by spraying 2% (wt/vol) 5-methylresorcinol in 2N sulfuric acid.

Online supplemental material

Fig. S1 shows the image of YFP-$GRAM_{Atg26}$ fluorescence along with that of a Golgi-specific marker. Fig. S2 shows the images of fluorescence from CFP-PpAtg26 variants along with YFP-PpAtg8 fluorescence. Fig. S3 provides the result of thin-layer chromatography of the total lipid extract from the CFP-PpAtg26 variant-harboring strains used in Fig. 4. Online supplemental material is available at http://www.jcb.org/cgi/content/full/jcb.200512142/DC1.

We thank Y. Ohsumi, N. Kato, H. Yurimoto, and H. Mukaiyama for their encouragement and helpful discussions; K. Takegawa for technical advice on phosphoinositide quantification; and D. Warnecke for providing ergosterol glucoside.

This research was founded by a grant-in-aid for Scientific Research on Priority Areas 399 (17028026) and 504 (16044223); a grant-in-aid for Scientific Research (S) (13854008); a grant from the Center of Excellence program from the Ministry of Education, Culture, Sports, Science and Technology of Japan; and a grant from the National Institute for Basic Biology Cooperative Research Program (to Y. Sakai).

The authors declare that they have no competing financial interests.

Submitted: 27 December 2005
Accepted: 1 May 2006

References

Abeliovich, H., T. Darsow, and S.D. Emr. 1999. Cytoplasm to vacuole trafficking of aminopeptidase I requires a t-SNARE-Sec1p complex composed of Tlg2p and Vps45p. *EMBO J.* 18:6005–6016.

Ano, Y., T. Hattori, M. Oku, H. Mukaiyama, M. Baba, Y. Ohsumi, N. Kato, and Y. Sakai. 2005. A sorting nexin PpAtg24 regulates vacuolar membrane dynamics during pexophagy via binding to phosphatidylinositol-3-phosphate. *Mol. Biol. Cell.* 16:446–457.

Audhya, A., M. Foti, and S.D. Emr. 2000. Distinct roles for the yeast phosphatidylinositol 4-kinases, Stt4p and Pik1p, in secretion, cell growth, and organelle membrane dynamics. *Mol. Biol. Cell.* 11:2673–2689.

Berger, P., C. Schaffitzel, I. Berger, N. Ban, and U. Suter. 2003. Membrane association of myotubularin-related protein 2 is mediated by a pleckstrin homology-GRAM domain and a coiled-coil dimerization module. *Proc. Natl. Acad. Sci. USA.* 100:12177–12182.

De Matteis, M.A., and A. Godi. 2004. PI-loting membrane traffic. *Nat. Cell Biol.* 6:487–492.

Doerks, T., M. Strauss, M. Brendel, and P. Bork. 2000. GRAM, a novel domain in glucosyltransferases, myotubularins and other putative membrane-associated proteins. *Trends Biochem. Sci.* 25:483–485.

Farre, J.C., and S. Subramani. 2004. Peroxisome turnover by micropexophagy: an autophagy-related process. *Trends Cell Biol.* 14:515–523.

Hamasaki, M., T. Noda, and Y. Ohsumi. 2003. The early secretory pathway contributes to autophagy in yeast. *Cell Struct. Funct.* 28:49–54.

Han, G.S., A. Audhya, D.J. Markley, S.D. Emr, and G.M. Carman. 2002. The *Saccharomyces cerevisiae* LSB6 gene encodes phosphatidylinositol 4-kinase activity. *J. Biol. Chem.* 277:47709–47718.

Hanada, K., K. Kumagai, S. Yasuda, Y. Miura, M. Kawano, M. Fukasawa, and M. Nishijima. 2003. Molecular machinery for non-vesicular trafficking of ceramide. *Nature.* 426:803–809.

Kihara, A., T. Noda, N. Ishihara, and Y. Ohsumi. 2001. Two distinct Vps34 phosphatidylinositol 3-kinase complexes function in autophagy and carboxypeptidase Y sorting in *Saccharomyces cerevisiae*. *J. Cell Biol.* 152:519–530.

Levine, T.P., and S. Munro. 2002. Targeting of Golgi-specific pleckstrin homology domains involves both PtdIns 4-kinase-dependent and -independent components. *Curr. Biol.* 12:695–704.

Mukaiyama, H., M. Oku, M. Baba, T. Samizo, A.T. Hammond, B.S. Glick, N. Kato, and Y. Sakai. 2002. Paz2 and 13 other PAZ gene products regulate vacuolar engulfment of peroxisomes during micropexophagy. *Genes Cells.* 7:75–90.

Mukaiyama, H., M. Baba, M. Osumi, S. Aoyagi, N. Kato, Y. Ohsumi, and Y. Sakai. 2004. Modification of a ubiquitin-like protein Paz2 conducted micropexophagy through formation of a novel membrane structure. *Mol. Biol. Cell.* 15:58–70.

Nakagawa, I., A. Amano, N. Mizushima, A. Yamamoto, H. Yamaguchi, T. Kamimoto, A. Nara, J. Funao, M. Nakata, K. Tsuda, et al. 2004. Autophagy defends cells against invading group A *Streptococcus*. *Science.* 306:1037–1040.

Nice, D.C., T.K. Sato, P.E. Stromhaug, S.D. Emr, and D.J. Klionsky. 2002. Cooperative binding of the cytoplasm to vacuole targeting pathway proteins, Cvt13 and Cvt20, to phosphatidylinositol 3-phosphate at the preautophagosomal structure is required for selective autophagy. *J. Biol. Chem.* 277:30198–30207.

Noda, T., J. Kim, W.P. Huang, M. Baba, C. Tokunaga, Y. Ohsumi, and D.J. Klionsky. 2000. Apg9p/Cvt7p is an integral membrane protein required for transport vesicle formation in the Cvt and autophagy pathways. *J. Cell Biol.* 148:465–480.

Noda, T., K. Suzuki, and Y. Ohsumi. 2002. Yeast autophagosomes: de novo formation of a membrane structure. *Trends Cell Biol.* 12:231–235.

Oku, M., D. Warnecke, T. Noda, F. Müller, E. Heinz, H. Mukaiyama, N. Kato, and Y. Sakai. 2003. Peroxisome degradation requires catalytically active sterol glucosyltransferase with a GRAM domain. *EMBO J.* 22:3231–3241.

Raiborg, C., T.E. Rusten, and H. Stenmark. 2003. Protein sorting into multivesicular endosomes. *Curr. Opin. Cell Biol.* 15:446–455.

Reggiori, F., C.W. Wang, U. Nair, T. Shintani, H. Abeliovich, and D.J. Klionsky. 2004. Early stages of the secretory pathway, but not endosomes, are required for Cvt vesicle and autophagosome assembly in *Saccharomyces cerevisiae*. *Mol. Biol. Cell.* 15:2189–2204.

Roth, M.G. 2004. Phosphoinositides in constitutive membrane traffic. *Physiol. Rev.* 84:699–730.

Sakai, Y., A. Koller, L.K. Rangell, G.A. Keller, and S. Subramani. 1998. Peroxisome degradation by microautophagy in *Pichia pastoris*: identification of specific steps and morphological intermediates. *J. Cell Biol.* 141:625–636.

Sciorra, V.A., A. Audhya, A.B. Parsons, N. Segev, C. Boone, and S.D. Emr. 2005. Synthetic genetic array analysis of the PtdIns 4-kinase Pik1p identifies components in a Golgi-specific Ypt31/rab-GTPase signaling pathway. *Mol. Biol. Cell.* 16:776–793.

Stolz, L.E., W.J. Kuo, J. Longchamps, M.K. Sekhon, and J.D. York. 1998. INP51, a yeast inositol polyphosphate 5-phosphatase required for phosphatidylinositol 4,5-bisphosphate homeostasis and whose absence confers a cold-resistant phenotype. *J. Biol. Chem.* 273:11852–11861.

Suzuki, K., T. Kirisako, Y. Kamada, N. Mizushima, T. Noda, and Y. Ohsumi. 2001. The pre-autophagosomal structure organized by concerted

functions of APG genes is essential for autophagosome formation. *EMBO J.* 20:5971–5981.

Tsujita, K., T. Itoh, T. Ijuin, A. Yamamoto, A. Shisheva, J. Laporte, and T. Takenawa. 2004. Myotubularin regulates the function of the late endosome through the GRAM domain-phosphatidylinositol 3,5-bisphosphate interaction. *J. Biol. Chem.* 279:13817–13824.

Tuttle, D.L., and W.A. Dunn Jr. 1995. Divergent modes of autophagy in the methylotrophic yeast *Pichia pastoris*. *J. Cell Sci.* 108:25–35.

Walch-Solimena, C., and P. Novick. 1999. The yeast phosphatidylinositol-4-OH kinase Pik1 regulates secretion at the Golgi. *Nat. Cell Biol.* 1:523–525.

Warnecke, D., R. Erdmann, A. Fahl, B. Hube, F. Müller, T. Zank, U. Zahringer, and E. Heinz. 1999. Cloning and functional expression of UGT genes encoding sterol glucosyltransferases from *Saccharomyces cerevisiae*, *Candida albicans*, *Pichia pastoris*, and *Dictyostelium discoideum*. *J. Biol. Chem.* 274:13048–13059.

Wurmser, A.E., and S.D. Emr. 2002. Novel PtdIns(3)P-binding protein Etf1 functions as an effector of the Vps34 PtdIns 3-kinase in autophagy. *J. Cell Biol.* 158:761–772.